SLAC-PUB-452
July 1968
(TH)

REGGE POLE EXCHANGE MODELS FOR HIGH ENERGY πN, NN, and $\overline{N}N$ ELASTIC SCATTERING†

V. Barger*
Stanford Linear Accelerator Center,
Stanford University, Stanford, California

(Talk given at the 1968 Institute for Theoretical Physics at the University of Colorado, Boulder, Colorado.)

†Supported in part by the University of Wisconsin Research Committee, with funds granted by the Wisconsin Alumni Research Foundation, and in part by the U. S. Atomic Energy Commission.

*Permanent Address: Physics Department, University of Wisconsin, Madison, Wisconsin.

I. INTRODUCTION

Experimental studies of $\pi^{\pm}p$, pp, and $\bar{p}p$ elastic processes over the last couple years have revealed the presence of dramatic structure in the scattering angular distributions at high energy. In particular these elastic differential cross sections show the following distinctive characteristics[1]:

ANGULAR REGION	CROSS SECTION	FEATURES
BACKWARD SCATTERING	$\frac{d\sigma}{du}(\pi^- p)$	smooth
	$\frac{d\sigma}{du}(\pi^+ p)$	dip at $u \simeq -0.15\,(\mathrm{BeV/c})^2$
FORWARD SCATTERING	$\frac{d\sigma}{dt}(\pi^{\pm} p)$	dips at $t \simeq -0.8$ and $t \simeq -2.7\,(\mathrm{BeV/c})^2$
	$\frac{d\sigma}{dt}(pp)$	nearly smooth
	$\frac{d\sigma}{dt}(\bar{p}p)$	dips at $t \simeq -0.5$ and $t \simeq -1.8\,(\mathrm{BeV/c})^2$

The minima and maxima in the angular distributions persist at energies above the resonance region, indicating an origin in the peripheral exchange mechanisms:

forward scattering $\longrightarrow$ meson exchanges

backward scattering $\longrightarrow$ baryon exchanges

In Regge pole exchange models, minima in scattering amplitudes can generally occur at momentum transfers for which a meson trajectory crosses

$$\alpha(t) = 0,\ -1,\ -2,\ \ldots$$

or a baryon trajectory intersects

$$\alpha(\sqrt{u}) = -1/2, \ -3/2, \ -5/2, \ \ldots \qquad .$$

Possible interpretations of the elastic scattering structures in terms of such exceptional points on Regge trajectories will be discussed in the following sections. In some cases adequate (but not necessarily unique) quantitative explanations of the elastic scattering data have already been possible. For other cases the Regge models are speculative and subject to modification as experimental information becomes more complete.

II. πN BACKWARD SCATTERING

The spirit of Regge models is to associate the exchange trajectories with the observed particle spectrum insofar as possible. The dominant πN resonances can be assigned to three leading fermion trajectories as shown in the Chew-Frautschi plot of Fig. II.1.[2] The signature (τ), parity (P), and isospin (I) quantum numbers of these trajectories are:

	$\tau=(-)^{J-1/2}$	P	I
N_α	+1	+	1/2
Δ_δ	-1	+	3/2
N_γ	-1	-	1/2

The striking feature of the trajectories is an indication for approximate straight lines in u, i.e., $(\text{mass})^2$.

$$\text{Real} \qquad \alpha(\sqrt{u}) \simeq a + bu$$

A complication is introduced in the fermion Regge exchange description of backward πN scattering by analyticity requirements. An unavoidable consequence of analyticity for the πN scattering amplitudes is the occurrence of fermion Regge trajectories in pairs that have opposite parity and join at $u = 0$. Using the notation $\alpha^{(\tau P)}(\sqrt{u})$ for the trajectories, the Gribov-MacDowell symmetry condition is

$$\alpha^{-}(\sqrt{u}) = \alpha^{+}(-\sqrt{u})$$

$$\beta^{-}(\sqrt{u}) = -\beta^{+}(-\sqrt{u})$$

for the trajectories and residues of these opposite parity poles.[3] Such a relationship at $u = 0$ is usually called a "conspiracy."

The doubling of trajectories does not necessarily require fermion recurrences of both parities. With an asymmetric $\sqrt{u}$ functional dependence, $\alpha^{+}(\sqrt{u})$ could intersect physical J values without $\alpha^{-}(\sqrt{u})$ doing so.

Nevertheless, a particularly interesting possibility is that particle recurrences are realized for both the α^{+} and α^{-} trajectories. Figure II. 2 shows tentative particle assignments to MacDowell symmetric (α, β) octet trajectories.[4] The occurrence of N_{α} (1688, $J^P = 5/2^+$) and N_{β}(1650, $J^P = 5/2^-$) resonances at about the same mass is especially suggestive of approximately MacDowell symmetric states. The nonexistence of an $I = 1/2$, $J^P = 1/2^-$ particle with mass ~ 1 BeV requires that the N_{β} trajectory choose nonsense at $\alpha^{-}(\sqrt{u}) = 1/2$ in order that the residue $\gamma^{-}(\sqrt{u})$ vanish there. This speculation can be directly tested by analysis of backward πN scattering data.

With these preliminaries, we turn to the description of the πN backward scattering data. When kinematical factors of order $1/s$ are neglected (an approximation that is not advisable in actual data fitting), the contribution of a MacDowell trajectory pair to the differential cross section for $u \leq 0$ has the form

$$\frac{d\sigma}{du} = \frac{1}{32\pi}\left\{\left|\gamma^{+}(\sqrt{u})\, R\left(\alpha^{+}(\sqrt{u}),\ s\right)\right|^2 + \left|\gamma^{-}(\sqrt{u})\, R\left(\alpha^{-}(\sqrt{u}),\ s\right)\right|^2\right\},$$

where

$$R\left(\alpha(\sqrt{u}),\ s\right) = \frac{1}{\Gamma(\alpha+1/2)}\ \frac{1+\tau e^{-i\pi(\alpha-1/2)}}{\sin\pi(\alpha-1/2)}\ \left(\frac{s-t}{2\,s_0}\right)^{\alpha-1/2}$$

At $u = 0$ the conspiring trajectories make equal contributions to $d\sigma/du$. The factor $R(\alpha, s)$ displays the usual Regge characteristics:

(i) The energy dependence is determined by α.

(ii) The phase is specified by α and the signature quantum number τ.

(iii) R vanishes at wrong signature, nonsense values of α.[5] (A wrong signature point for a fermion trajectory is an half-integral value of α at which $(-)^{\alpha-1/2} = -\tau$; nonsense means that the corresponding angular momentum value is unphysical for the helicity amplitudes.) This property of the Regge amplitude assumes the absence of fixed poles, or equivalently, that the third double spectral function is negligible.[6]

Property (iii) is essential to the Regge explanation of the dip in π^+p backward scattering. Since $\sqrt{u}$ becomes imaginary in the scattering region, the Regge amplitude will have an appreciable dip near a wrong signature nonsense point only if the trajectory is approximately an even function of $\sqrt{u}$. For the linear trajectories of Fig. II. 1, the u values of the wrong signature nonsense points are

N_α	$\alpha = -1/2$	$u \approx -0.11(\mathrm{BeV}/c)^2$
Δ_δ	$\alpha = -3/2$	$u \approx -1.8$
$N\gamma$	$\alpha = -3/2$	$u \approx -0.7$ (uncertain trajectory form)

The isotopic spin relations

$$f(\pi^- p) = f(\Delta)$$

$$f(\pi^+ p) = \frac{1}{3}\,[f(\Delta) + 2f(N)]$$

$$f(\pi^- p \rightarrow \pi^0 n) = \frac{\sqrt{2}}{3}\,[f(N) - f(\Delta)]$$

are used in adding up the $\Delta(I = 3/2)$ and $N(I = 1/2)$ fermion Regge exchange contributions to the πN elastic and charge exchange amplitudes. Some qualitative conclusions regarding the N and Δ amplitudes can be made directly from the experimental data[7] on $d\sigma/du\ (\pi^{\pm} p)$ at 9.9 BeV/c shown in Fig. II.3. At the backward direction $(u \simeq +0.03)$, the ratio

$$\frac{d\sigma}{du}(\pi^+ p) \Big/ \frac{d\sigma}{du}(\pi^- p) \approx 4$$

indicates the dominance of N exchanges. Away from 180°, $d\sigma/du(\pi^+ p)$ drops precipitiously and the ratio is consistent with

$$\frac{d\sigma}{du}(\pi^+ p) \Big/ \frac{d\sigma}{du}(\pi^- p) \approx 1/9$$

at $u \simeq -0.15\,(\mathrm{BeV/c})^2$, suggesting a zero of the N exchange amplitude at this u-value. These qualitative features are readily reproduced by an $N_\alpha + \Delta_\delta$ exchange model. The N_α amplitude zero at $\alpha = -1/2$ accounts for the $\pi^+ p$ dip. In this picture the N_α trajectory can be allowed no appreciable $\sqrt{u}$ term and the N_γ amplitude contribution necessarily must be small.

Quantitative fits to high energy data on $d\sigma/du\ (\pi^{\pm} p)$[7] using a Regge model with linear N_α and Δ_δ trajectories of the form $\alpha(\sqrt{u}) = a + bu$ are shown by the solid curves in Figs. II.4 and II.5.[8] The trajectory parameters obtained from this fit to the scattering data were

$$N_\alpha: \qquad \alpha = -0.38 + 0.88\ u$$

$$\Delta_\delta: \qquad \alpha = +0.19 + 0.87\ u \quad .$$

These parameters are in excellent agreement with the values obtained from the Chew-Frautschi plot of the πN resonances:

$$N_\alpha: \qquad \mathrm{Re}\ \alpha = -0.39 + 1.0\ u$$

$$\Delta_\delta: \qquad \mathrm{Re}\ \alpha = +0.15 + 0.9\ u$$

The above results quantitatively substantiate the connection between the particle mass spectra and the particle exchange amplitudes, as expressed by the Regge trajectory functions.

The principle defect of the above fit is a predicted dip in $d\sigma/du\ (\pi^- p)$ at $u \simeq -1.9$ corresponding to $\alpha_\Delta = -3/2$. A possible explanation for the experimental absence of this dip is a leveling off of the Δ_δ trajectory at large $|u|$. The dashed curves in Fig. II.5 illustrate results obtained with

$$\alpha = \frac{0.21 + 0.9\ u}{1 - 1.6\ u}$$

for the Δ_δ trajectory. Measurements of the energy dependence of $d\sigma/du$ at large $|u|$ will be necessary to answer this interesting question regarding the behavior of the trajectories at large $|u|$.[9]

For the above fits the N_α and Δ_δ residues were parameterized as

$$\gamma_N^+(\sqrt{u}) = \beta_N(1 + \delta_N \sqrt{u})$$

$$\gamma_\Delta^-(\sqrt{u}) = \beta_\Delta(1 + \delta_\Delta \sqrt{u})$$

where the β_i and δ_i are constants. For approximately linear trajectories we expect $\delta_N \approx 1/M_N$ and $\delta_\Delta \approx 1/M_\Delta$ on the basis of the absence of the lowest lying particles on MacDowell reflected trajectories. The values obtained from the fits were $\delta_N = 1.6/M_N$ and $\delta_\Delta = 1.5/M_\Delta$. It is encouraging that the πN scattering data require positive δ's with roughly the expected magnitudes.

The Reggeized baryon exchange amplitudes which describe the high energy data also correctly extrapolate through the mean value of the $\pi^+ p$ differential cross sections down to 2 BeV/c, as shown by the solid curves in Figs. II.6 and II.7.[10] Superimposed on the mean behavior are oscillations associated with direct channel resonances. The Regge predictions for the mean values of $d\sigma/du$ ($\pi^- p \to \pi^0 n$) are shown in Fig. II.8. The charge exchange cross section is sensitive to the sign of β_N/β_Δ, which is not determined by fits to the present $\pi^\pm p$ scattering data. The solid curves in Fig. II.8 correspond to $\beta_\Delta/\beta_N < 0$ and the dashed curves to $\beta_\Delta/\beta_N > 0$. Extrapolation to the N_α (938, $1/2^+$) and Δ_δ (1236, $3/2^+$) particle poles gives $\beta_\Delta/\beta_N < 0$. Accurate $\pi^- p \to \pi^0 n$ data in the 2-5 BeV/c region should resolve this sign ambiguity and provide a further critical test on the validity of the $N_\alpha + \Delta_\delta$ exchange model. At high energy a dip in $d\sigma/du$ ($\pi^- p \to \pi^0 n$) at fixed $u \simeq -0.15$ (BeV/c)^2 is predicted from the N_α amplitude zero at $\alpha = -1/2$.[11]

III. FORWARD ELASTIC SCATTERING

The Regge pole description of high energy elastic scattering in the forward hemisphere is complicated by the number of meson trajectories that are allowed as exchanges. At the present stage of development the Regge models of elastic amplitudes are decidedly non-unique. Nevertheless the prominent aspects of the elastic data can be interpreted in the Regge pole framework.[12]

In Fig. III. 1 the qualitative features of the πN, NN, and $\overline{N}N$ elastic and charge exchange data are displayed at $P_{LAB} \sim 3$ BeV/c. The $d\sigma/dt$ (pp) data are smooth and the $d\sigma/dt$ ($\bar{p}p$) data go through a deep minimum at $t \simeq -0.5 (\mathrm{BeV/c})^2$. The $d\sigma/dt$ (π^+p) and $d\sigma/dt$ (π^-p) data have roughly the same shape with a change in slope at $t \simeq -0.8$ $(\mathrm{BeV/c})^2$; at lower momenta a dip is observed in $d\sigma/dt\,(\pi^{\pm}p)$ at this t-value. The change in sign of the differences

$$\left[\frac{d\sigma}{dt}\,(\overline{A}B) - \frac{d\sigma}{dt}\,(AB)\right]$$

at $t \simeq -0.15$ $(\mathrm{BeV/c})^2$ can be observed in the data. The interpretation of this "crossover" phenomenon in Regge models is an involved subject[13] and will not be discussed here.

The construction of meson exchange models for the elastic data is somewhat simplified by the approximate isospin independence equalities[1]:

$$\frac{d\sigma}{dt}\,(\pi^+p) \simeq \frac{d\sigma}{dt}\,(\pi^-p)$$

$$\frac{d\sigma}{dt}\,(pp) \simeq \frac{d\sigma}{dt}\,(np)$$

On this basis we conclude that $I = 0$ exchanges dominate the high energy elastic scattering differential cross sections. The usual Regge models use P, P', and ω $I = 0$ exchanges. Speculative shapes for these trajectories are shown in Fig. III. 2.[14] The Pomeranchuk trajectory (P) is known to be rather flat while the P' and ω trajectories appear to have normal slopes $\sim 1(\mathrm{BeV/c})^{-2}$, at least for small t.

The Regge interpretation of the elastic dips at $t \approx -0.5$ $(\mathrm{BeV/c})^2$ is related to the behavior of the P' and ω residues at $\alpha = 0$. We begin with the construction of a simple model that reproduces the main features of the data. We use only spin-nonflip amplitudes, neglecting the small high energy polarizations. The scattering amplitudes then have the forms:

$$f_{\pi^+p} = f_{\pi^-p} = f_{\pi N}(P) + f_{\pi N}(P')$$

$$f_{pp} = f_{pn} = f_{NN}(P) + f_{NN}(P') + f_{NN}(\omega)$$

$$f_{\bar{p}p} = f_{\bar{p}n} = f_{NN}(P) + f_{NN}(P') - f_{NN}(\omega)$$

The normalization $d\sigma/dt = |f|^2$ will be used. Approximating the P' and ω by a single degenerate trajectory and taking $\alpha_P(t) \equiv 1$, the Regge amplitudes are

$$f(P) = \gamma i$$

$$f(P') = -\beta \frac{e^{-\frac{i\pi\alpha}{2}}}{\sin \frac{\pi\alpha}{2}} s^{\alpha-1}$$

$$f(\omega) = i\bar{\beta} \frac{e^{-\frac{i\pi\alpha}{2}}}{\cos \frac{\pi\alpha}{2}} s^{\alpha-1}$$

where $\gamma(t)$, $\beta(t)$, and $\bar{\beta}(t)$ are residues and $\alpha(t)$ the P'-ω trajectory. Subscripts πN and NN on the residues have been suppressed above. We now make the ansatz that the behavior of the residues in the t-range of interest is[14]

$$\beta(t) \approx \lambda(t) \sin^2 \frac{\pi\alpha}{2} \qquad (P' \text{ residue})$$

$$\bar{\beta}(t) \approx \lambda(t) \cos^2 \frac{\pi\alpha}{2} \qquad (\omega \text{ residue})$$

Effectively, we are assuming (a) the sense mechanism for ω and the no-compensation mechanism for P' at $\alpha = 0$; (b) correlated magnitudes of P' and ω residues. With this cyclic residue ansatz, the differential cross section expressions are

$$\frac{d\sigma}{dt}(\pi N) = \tilde{\gamma}^2 + \left[2\tilde{\gamma}\tilde{\lambda}\, s^{\alpha-1} + \tilde{\lambda}^2\, s^{2\alpha-2}\right] \sin^2 \frac{\pi\alpha}{2}$$

$$\frac{d\sigma}{dt}(NN) = \gamma^2 + 2\gamma\lambda\, s^{\alpha-1} + \lambda^2\, s^{2\alpha-2}$$

$$\frac{d\sigma}{dt}(\overline{N}N) = \gamma^2 - 2\gamma\lambda \cos \pi\alpha\, s^{\alpha-1} + \lambda^2\, s^{2\alpha-2}$$

In this qualitative model, dips occur in πN and $\overline{N}N$ at $\alpha = 0$ whereas NN is smooth as required. The dips come from terms that decrease rapidly as s increases.

A quantitative fit to the structure of the elastic differential cross sections has been made by Chiu, Chu, and Wang with a basicly similar model[15] (the same mechanisms at $\alpha = 0$ were employed, but the cyclic residue condition was not used). The results of this fit are compared with the scattering data in Figs. III. 3 and III. 4. The rapid fall with energy of the secondary bumps is apparent in the data.

Recent data on $\pi^{\pm}p$ and $\bar{p}p$ elastic scattering at larger momentum transfer reveal the presence of additional dips in the differential cross sections. The $\pi^{\pm}p$ data in Fig. III. 5 [16,17] have a second minimum at $t \simeq -2.7\ (\mathrm{BeV}/c)^2$. The approximate equality of π^+p and π^-p differential cross sections holds out to the second dip in the 3.5 BeV/c data, suggesting the continued dominance of $I = 0$ meson exchanges. The u-channel baryon exchanges presumably account for the deviation from equality beyond the second dip at this low momentum.

The energy dependences of the π^+p and π^-p data have been separately analyzed by Booth[17] in terms of a flat Pomeranchuk trajectory and another trajectory (the P' in our notation). The computed values of the P' trajectory are consistent with a linear form as shown in Fig. III.6. At the position of the second dip ($t \simeq -2.7$), the P' trajectory value is $\alpha_{P'} \approx -2$. At $\alpha_{P'} \simeq -1$ the data do not show the expected wrong signature nonsense dip. The experimental absence of the P' amplitude zero at $\alpha_{P'}(t) = -1$ may be due to a fixed pole in the residue at this t-value. However, a third double spectral function of sufficient strength to eliminate the P' amplitude zero might also have been expected to give rise to branch cuts that would produce deviations from a simple s^α energy dependence. The theoretical implications of these phenomenological results clearly deserve further attention. It is amusing to note that the cyclic P' residue structure discussed previously reproduces the correct empirical behavior of the πN differential cross sections at $\alpha_{P'} = -1$ and $\alpha_{P'} = -2$.

Representative data on pp and $\bar{p}p$ elastic scattering at large $|t|$ are plotted in Fig. III.7.[16,19] The $\bar{p}p$ data show dips at $t \simeq -0.5$ and $t \simeq -1.8$ $(\mathrm{BeV/c})^2$. $d\sigma/dt\,(\bar{p}p)$ lies below $d\sigma/dt\,(pp)$ for all $|t| \geq 0.2(\mathrm{BeV/c})^2$. A quantitative Regge analysis of this large t data has not yet been carried out.

The elastic scattering data have provided the first evidence for linearly falling meson trajectories in the region $|t| > 1(\mathrm{BeV/c})^2$. Further accumulation of data on elastic processes at high energy and large $|t|$ should provide valuable clues on the nature of the Regge dip mechanisms.

I thank Professor S. Drell for the hospitality of the SLAC theoretical group.

REFERENCES

1. A summary of the data can be found in the Proceedings of the Topical Conference on High Energy Collisions of Hadrons, CERN Report 68-7.
2. V. Barger and D. Cline, Phys. Rev. Letters 16, 913 (1966); Phys. Rev. 155, 1792 (1967).
3. V. N. Gribov, Soviet Physics JETP (USA) 16, 1080 (1963); S. W. MacDowell, Phys. Rev. 116, 774 (1959); V. Singh, Phys. Rev. 129, 1889 (1963).
4. V. Barger and D. Cline, Phys. Letters 26B, 83 (1967).
5. C. B. Chiu and J. D. Stack, Phys. Rev. 153, 1575 (1967).
6. S. Mandelstam and L. Wang, Phys. Rev. 160, 1490 (1967).
7. R. Rubinstein, A. Ashmore, C.J.S. Damerell, W. R. Frisken, J. Orear, D. P. Owen, F. C. Peterson, A. L. Read, D. G. Ryan, and D. H. White, Phys. Rev. Letters (to be published).
8. V. Barger and D. Cline, "Evidence for Linear Extrapolations of Baryon Exchange Trajectories Through Particle Mass Spectra," (to be published).
9. An appreciable $\sqrt{u}$ term in the Δ_δ trajectory could also wash out the $\alpha = -3/2$ dip. However, fits obtained with a large $\sqrt{u}$ dependence of α_Δ did not reproduce the data nearly as well.
10. V. Barger and D. Cline, "Prediction of the Mean Backward $\pi^- p \to \pi^0 n$ Differential Cross Section Down to 2.0 BeV/c," (to be published).
11. V. Barger and D. Cline, Phys. Rev. Letters 19, 1504 (1967).
12. A recent Regge pole fit to the elastic scattering data can be found in W. Rarita, R. Riddell, C. Chiu, and R. Phillips, Phys. Rev. 165, 1615 (1968).
13. V. Barger and L. Durand, III, Phys. Rev. Letters 19, 1295 (1967).
14. V. Barger and R. J. N. Phillips, Phys. Rev. Letters 20, 564 (1968).
15. C. Chiu, S. Chu, and L. Wang, Phys. Rev. 161, 1563 (1967).

16. J. Orear (private communication); A. Ashmore, C.J.S. Damerell, W. R. Frisken, R. Rubinstein, J. Orear, D. P. Owen, F. C. Peterson, A. L. Read, D. G. Ryan, and D. H. White, "High Energy π^-p, K^-p, and $\bar{p}p$ Elastic Scattering," (to be published).

17. C. T. Coffin, N. Dikmen, L. Ettlinger, D. Meyer, A. Saulys, K. Terwilliger, and D. Williams, Phys. Rev. Letters 17, 458 (1966); 15, 838 (1965).

18. N. E. Booth, University of Chicago preprint, EFI 68-28.

19. The sources for the pp data are listed on page 587 of Ref. 1.

FIGURE CAPTIONS

II. 1. Assignments of the dominant πN resonances to Regge trajectories. (Ref. 2.)

II. 2. Tentative assignments of resonances to parity doublets on MacDowell symmetric (α, β) octet trajectories. (Ref. 4.)

II. 3. Data on $\pi^{\pm}p$ backward elastic scattering at 9.9 BeV/c. (Ref. 7.) Interpolating curves are drawn through the data.

II. 4. N_{α}, Δ_{δ} linear Regge trajectory fits (Ref. 8) to $\pi^{+}p$ backward scattering data (Ref. 7) are shown by the solid curves.

II. 5. Δ_{δ} linear Regge trajectory fits (Ref. 8) to $\pi^{-}p$ backward scattering data (Ref. 7) are illustrated by the solid curves. The dashed curve represents a non-linear Δ_{δ} trajectory as discussed in the text.

II. 6. Extrapolation of $(N_{\alpha}, \Delta_{\delta})$ Regge exchange model for $\pi^{+}p$ backward scattering to intermediate energies. (Ref. 10.) Interpolating curves are drawn through the intermediate energy data.

II. 7. Extrapolation of Δ_{δ} Regge exchange model for $\pi^{-}p$ backward scattering to intermediate energies. (Ref. 10.)

II. 8. $(N_{\alpha}, \Delta_{\delta})$ Regge exchange model predictions for the $\pi^{-}p \rightarrow \pi^{0}n$ differential cross section. The solid curve represents to prediction with $\beta_{\Delta}/\beta_{N} < 0$ and the dashed curve the prediction for $\beta_{\Delta}/\beta_{N} > 0$. (Ref. 10.)

III. 1. Qualitative features of πN, NN, and $\overline{N}N$ elastic and charge exchange scattering data for $P_{LAB} \sim 3$ BeV/c.

III. 2. Speculative straight line P, P', and ω Regge trajectories (Ref. 14).

III. 3. $\pi^{\pm}p$ elastic scattering data. The curves represent a Regge pole fit with P, P', and ρ exchanges. (Ref. 15.)

III. 4. pp and $\overline{p}p$ elastic scattering data. The curves represent a fit with P, P', and ω Regge exchanges. (Ref. 15.)

III. 5. Structure in $\pi^{\pm}p$ elastic scattering at large momentum transfers. (Data from Refs. 16 and 17.)

III. 6. Values of P' trajectory deduced from the energy dependences of $\pi^{+}p$ and $\pi^{-}p$ differential cross sections. A two pole exchange model was assumed (P + P') with $\alpha_{P}(t) \equiv 1$. (Ref. 18.)

III. 7. Comparison of structure in $\bar{p}p$ elastic scattering data with pp data at similar momenta. (Data from Refs. 16 and 19.)

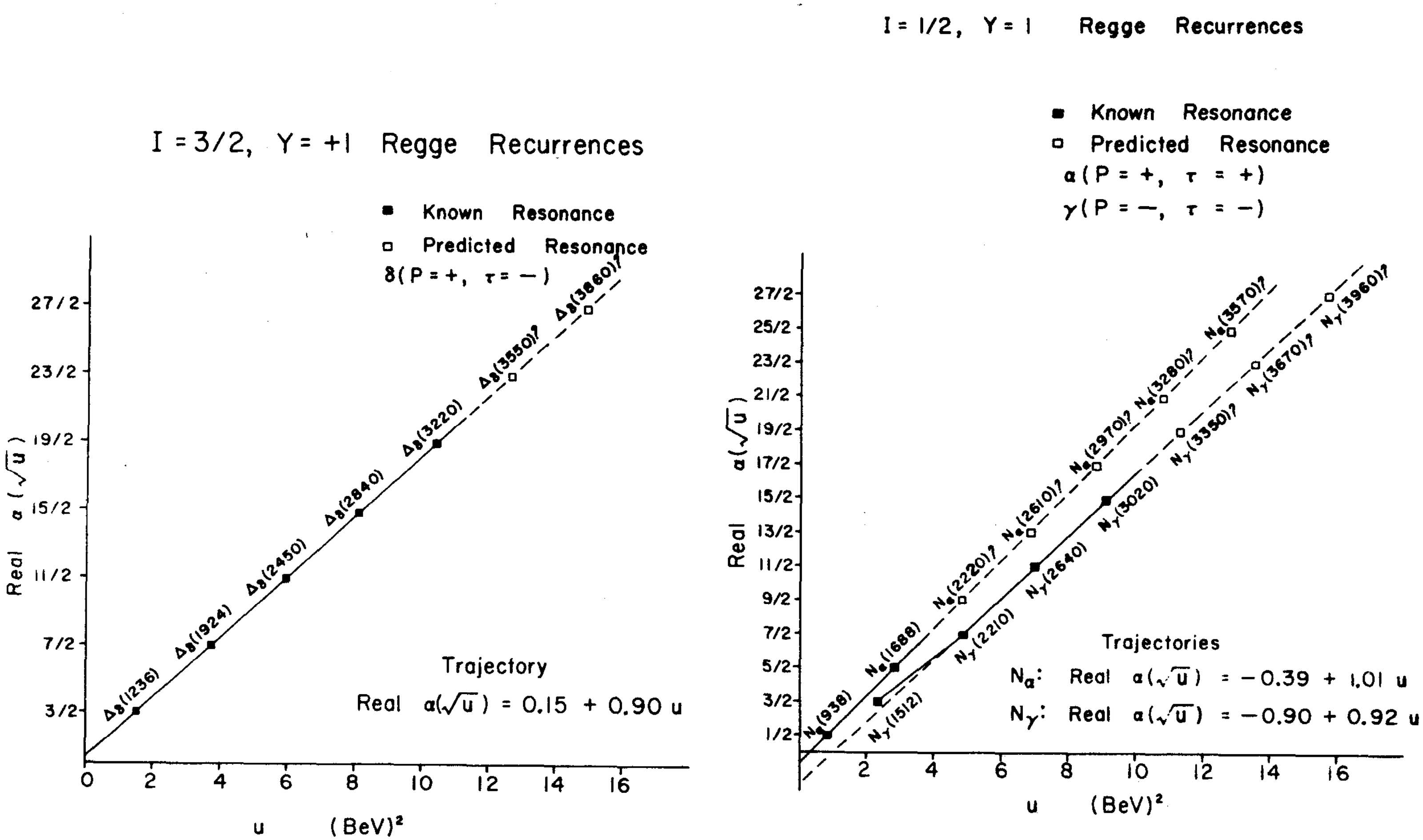
I = 3/2, Y = +1 Regge Recurrences
Known Resonance
Predicted Resonance
δ(P = +, τ = −)
Trajectory
Real α(√u) = 0.15 + 0.90 u
Real α(√u)
u (BeV)²
I = 1/2, Y = 1 Regge Recurrences
Known Resonance
Predicted Resonance
α(P = +, τ = +)
γ(P = −, τ = −)
Trajectories
Nα: Real α(√u) = −0.39 + 1.01 u
Nγ: Real α(√u) = −0.90 + 0.92 u
Real α(√u)
u (BeV)²

FIG. II. 1

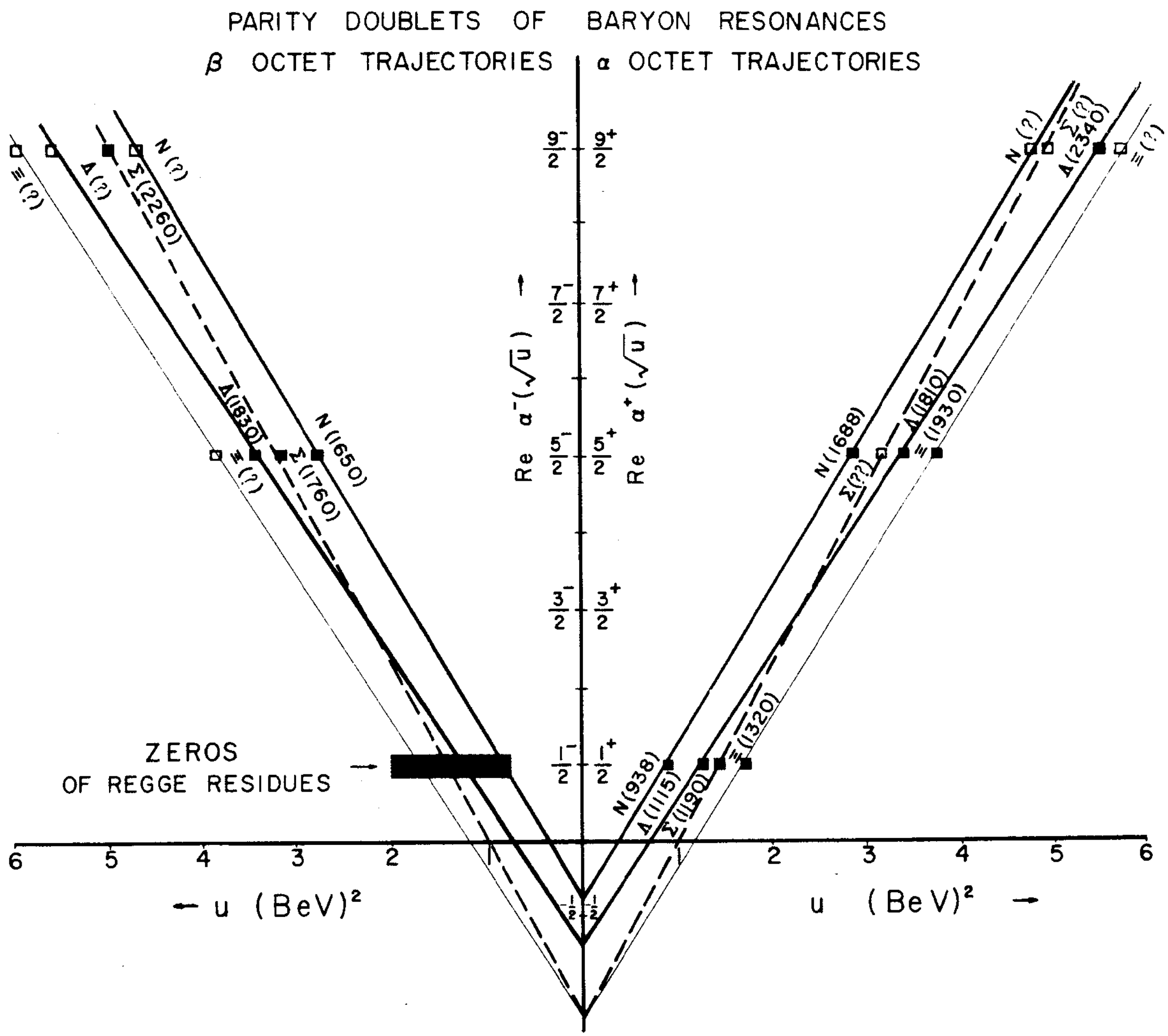
PARITY DOUBLETS OF BARYON RESONANCES
β OCTET TRAJECTORIES
α OCTET TRAJECTORIES
ZEROS
OF REGGE RESIDUES
Re $\alpha^-(\sqrt{u})$
Re $\alpha^+(\sqrt{u})$
← u (BeV)²
u (BeV)² →
N(1650)
Λ(1830)
Σ(1760)
Σ(2260)
N(938)
Λ(1115)
Σ(1190)
Ξ(1320)
N(1688)
Λ(1810)
Ξ(1930)
Λ(2340)

FIG. II.2

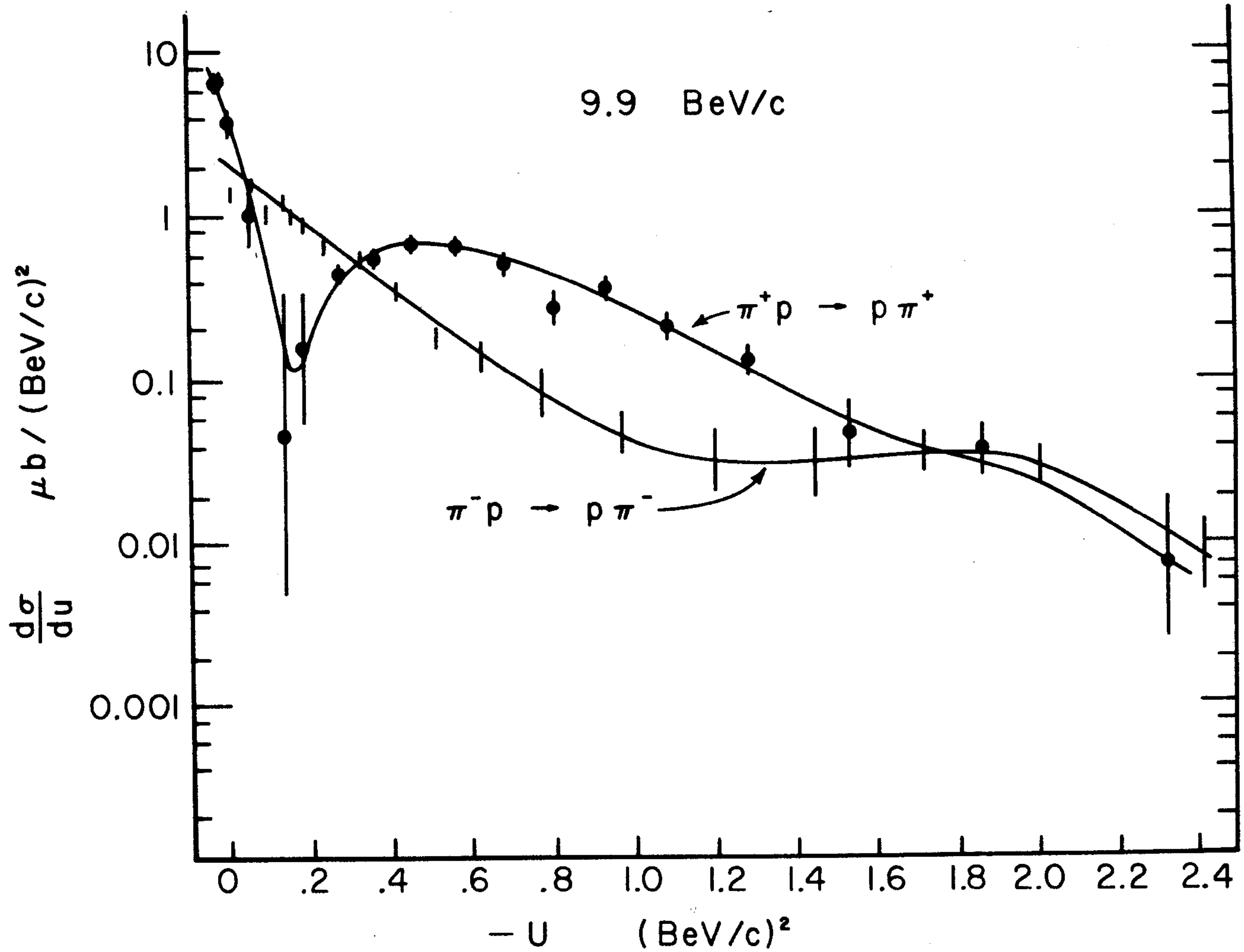

9.9 BeV/c
$\pi^+ p \rightarrow p \pi^+$
$\pi^- p \rightarrow p \pi^-$
$\frac{d\sigma}{du}$ $\mu b / (BeV/c)^2$
10
1
0.1
0.01
0.001
0
.2
.4
.6
.8
1.0
1.2
1.4
1.6
1.8
2.0
2.2
2.4
$-U$ $(BeV/c)^2$

FIG. II.3

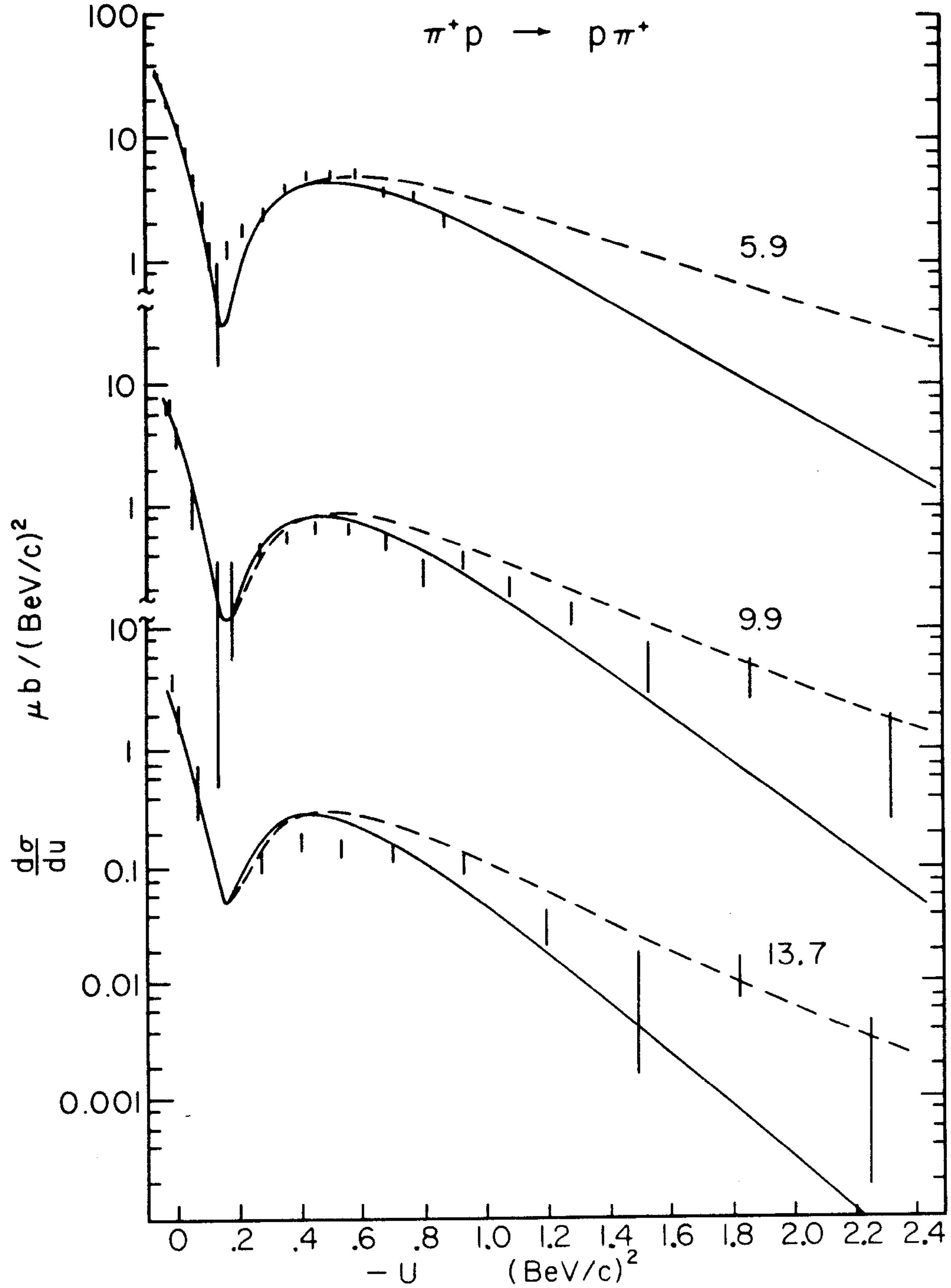

$\pi^+ p \rightarrow p \pi^+$
100
10
1
10
1
$10^{?}$
1
0.1
0.01
0.001
5.9
9.9
13.7
$\frac{d\sigma}{du}$ $\mu b / (BeV/c)^2$
0
.2
.4
.6
.8
1.0
1.2
1.4
1.6
1.8
2.0
2.2
2.4
$-U$ $(BeV/c)^2$

FIG. II.4

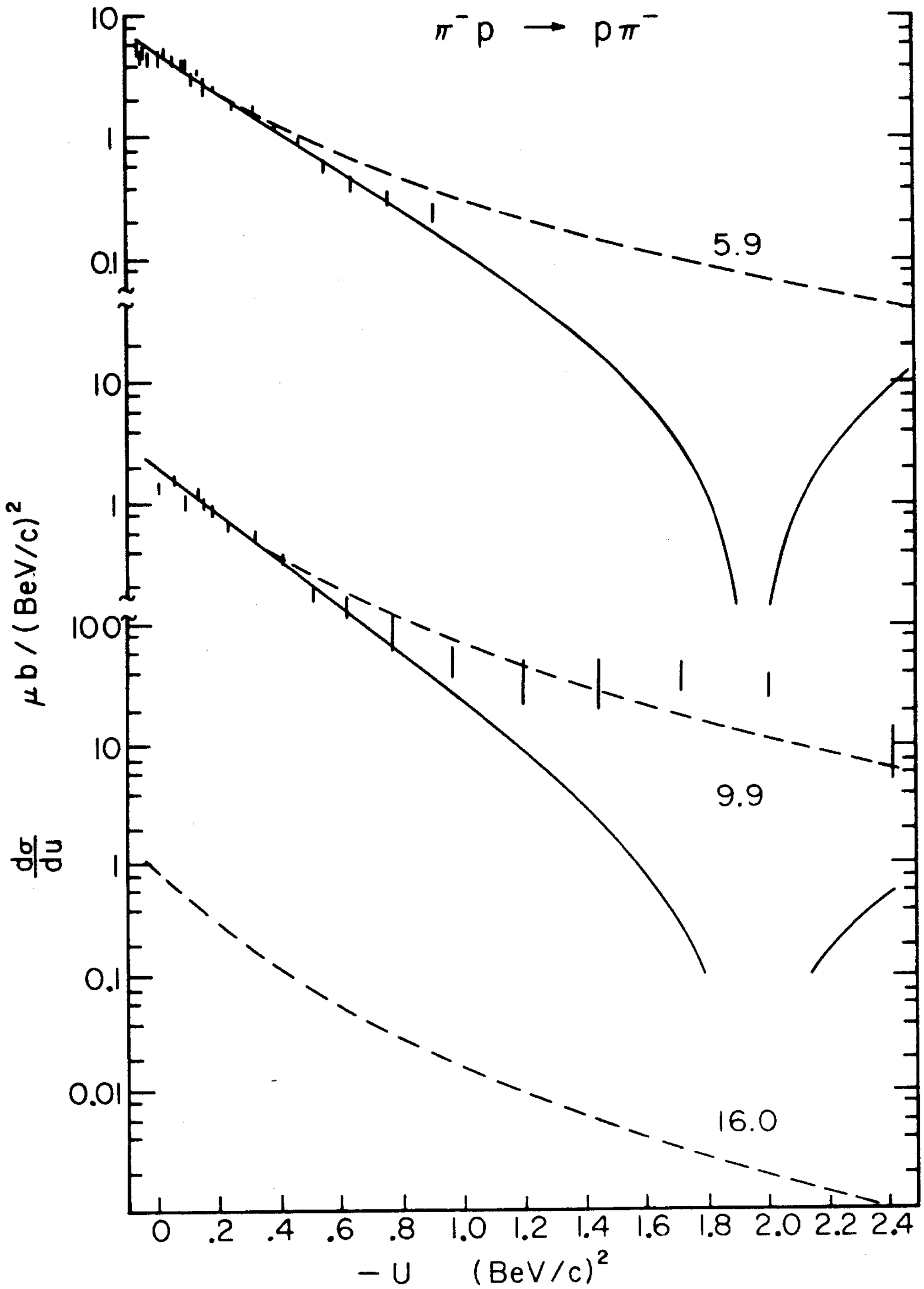

$\pi^- p \rightarrow p\pi^-$
5.9
9.9
16.0
$\frac{d\sigma}{du}$ $\mu b/(BeV/c)^2$
$-U \quad (BeV/c)^2$
10
1
0.1
10
1
100
10
1
0.1
0.01
0
.2
.4
.6
.8
1.0
1.2
1.4
1.6
1.8
2.0
2.2
2.4

FIG. II.5

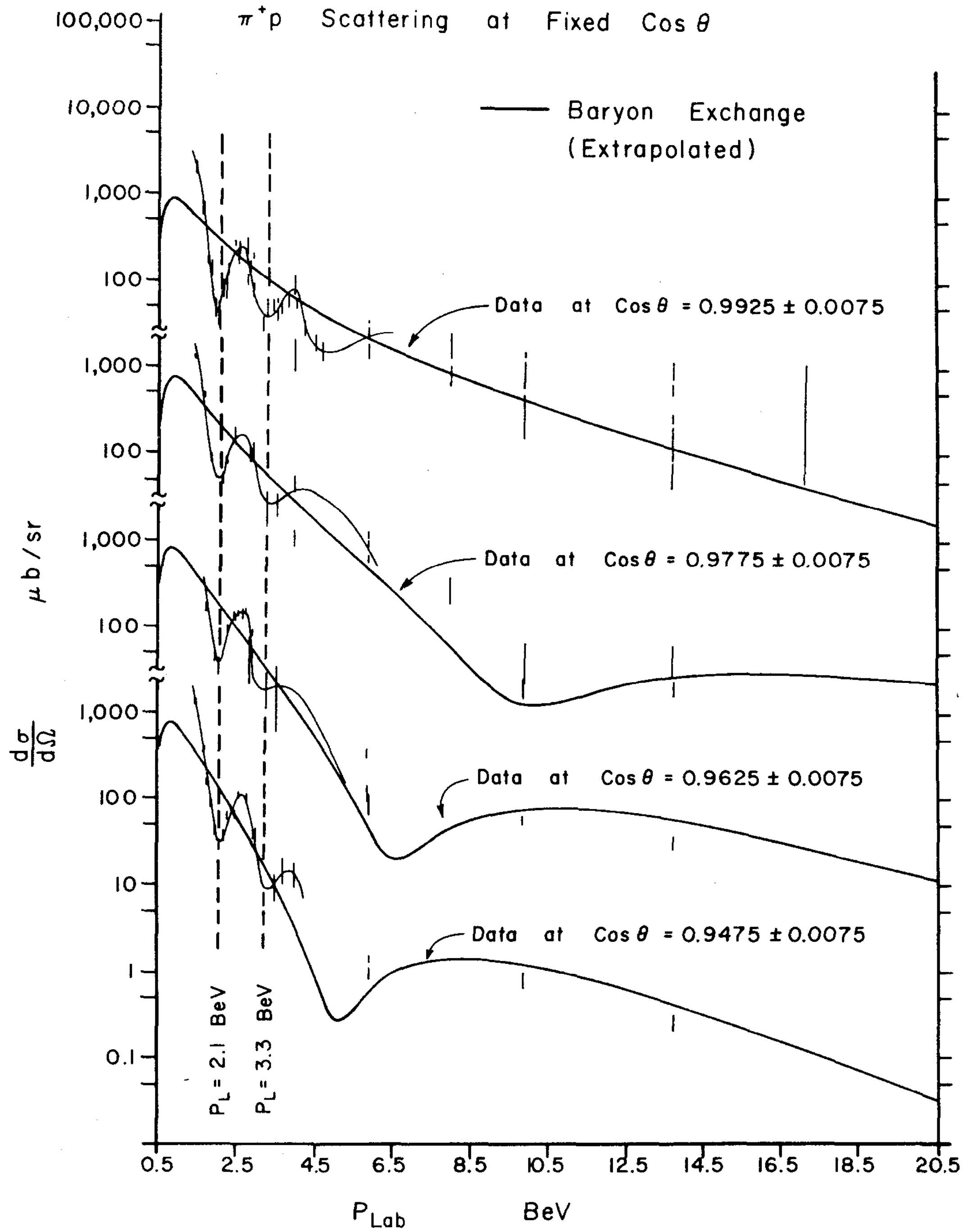

π⁺p Scattering at Fixed Cos θ
Baryon Exchange
(Extrapolated)
Data at Cos θ = 0.9925 ± 0.0075
Data at Cos θ = 0.9775 ± 0.0075
Data at Cos θ = 0.9625 ± 0.0075
Data at Cos θ = 0.9475 ± 0.0075
dσ/dΩ μb/sr
100,000
10,000
1,000
100
1,000
100
1,000
100
1,000
100
10
1
0.1
P_L = 2.1 BeV
P_L = 3.3 BeV
0.5
2.5
4.5
6.5
8.5
10.5
12.5
14.5
16.5
18.5
20.5
P_Lab BeV

FIG. II.6

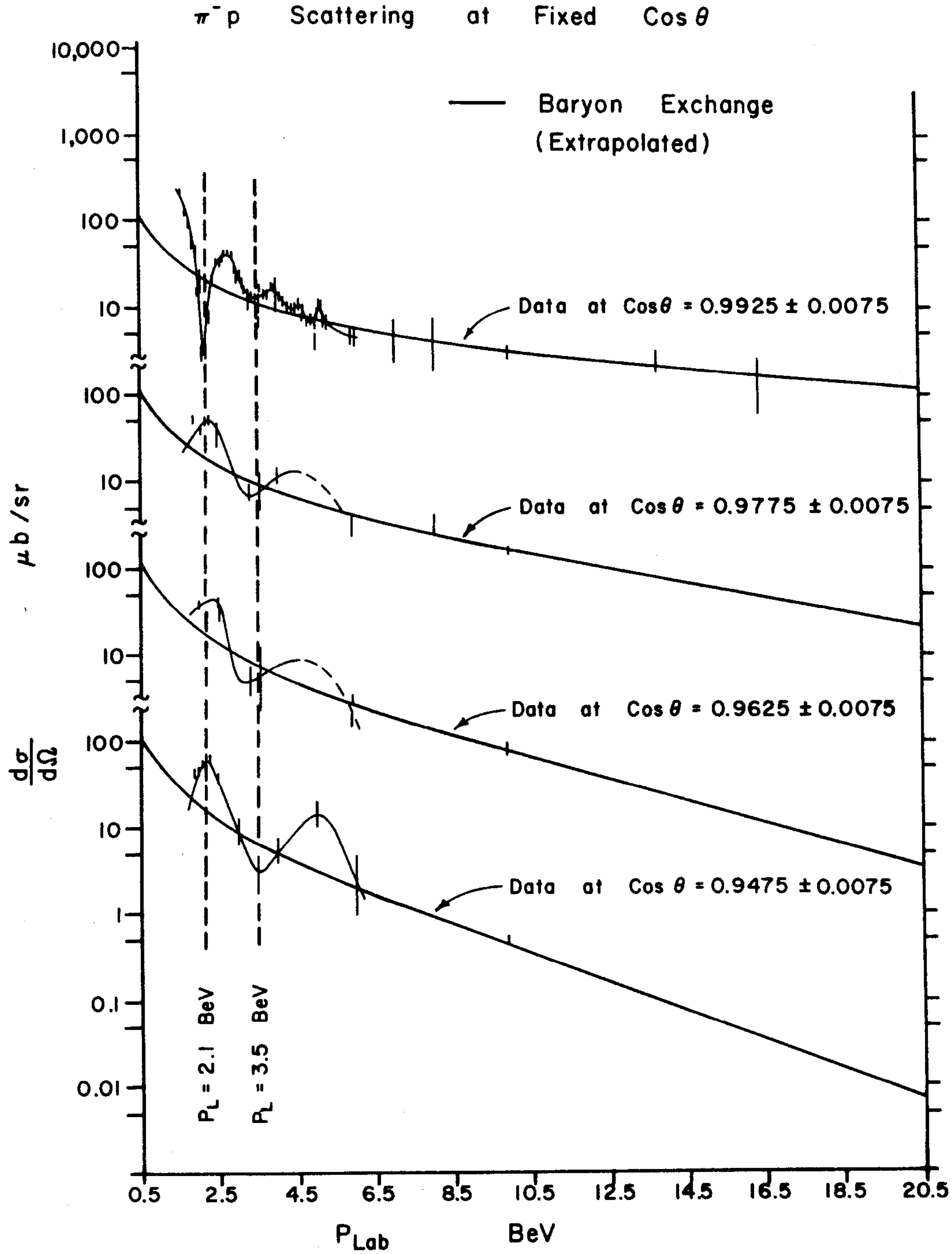

$\pi^- p$ Scattering at Fixed Cos θ
Baryon Exchange
(Extrapolated)
Data at Cos θ = 0.9925 ± 0.0075
Data at Cos θ = 0.9775 ± 0.0075
Data at Cos θ = 0.9625 ± 0.0075
Data at Cos θ = 0.9475 ± 0.0075
$\frac{d\sigma}{d\Omega}$ μb/sr
10,000
1,000
100
10
1
0.1
0.01
P_L = 2.1 BeV
P_L = 3.5 BeV
0.5
2.5
4.5
6.5
8.5
10.5
12.5
14.5
16.5
18.5
20.5
P_{Lab} BeV

FIG. II.7

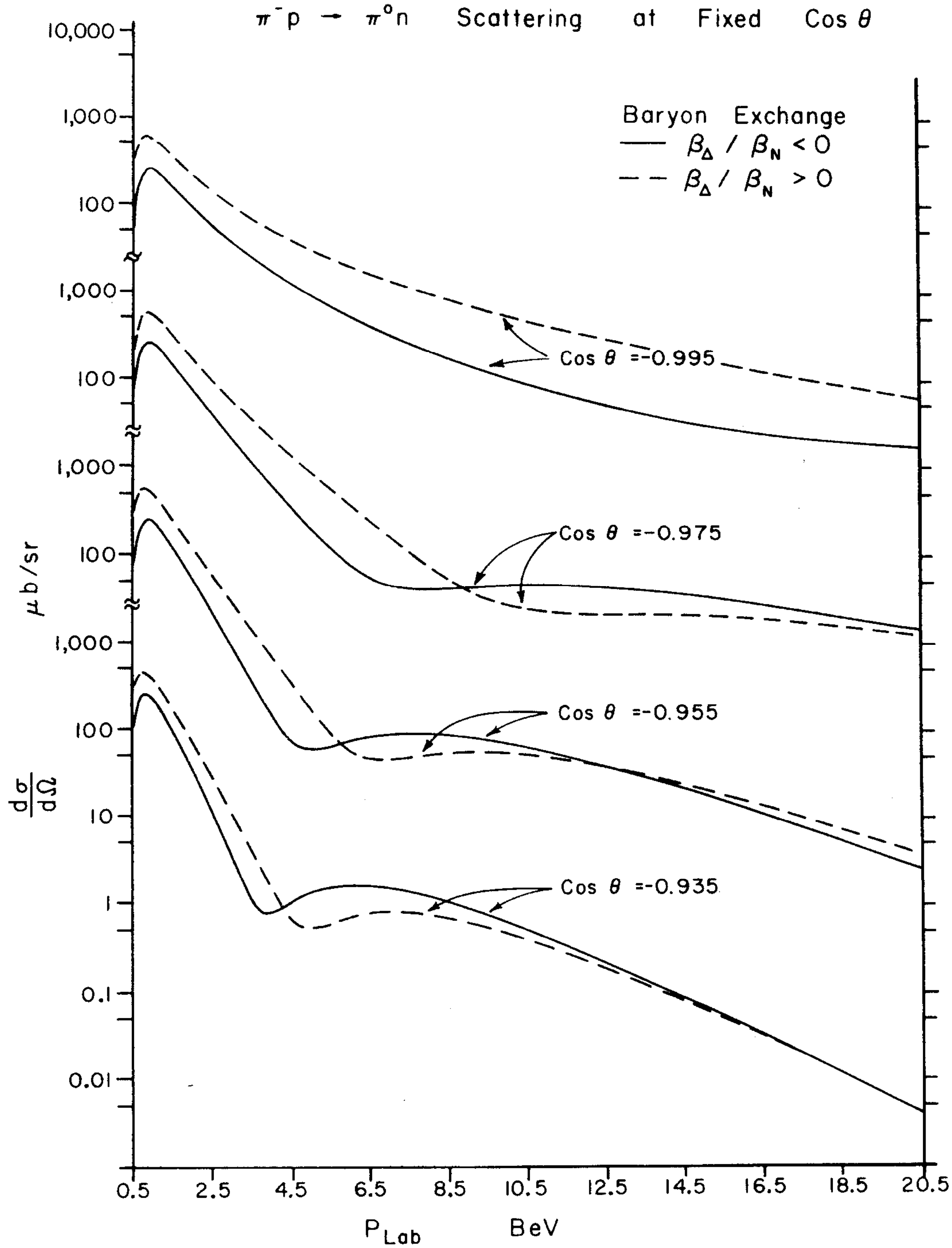

$\pi^- p \rightarrow \pi^\circ n$ Scattering at Fixed Cos θ
Baryon Exchange
$\beta_\Delta / \beta_N < 0$
$\beta_\Delta / \beta_N > 0$
Cos θ =-0.995
Cos θ =-0.975
Cos θ =-0.955
Cos θ =-0.935
$\frac{d\sigma}{d\Omega}$ μb/sr
10,000
1,000
100
10
1
0.1
0.01
0.5
2.5
4.5
6.5
8.5
10.5
12.5
14.5
16.5
18.5
20.5
P_{Lab} BeV

FIG. II.8

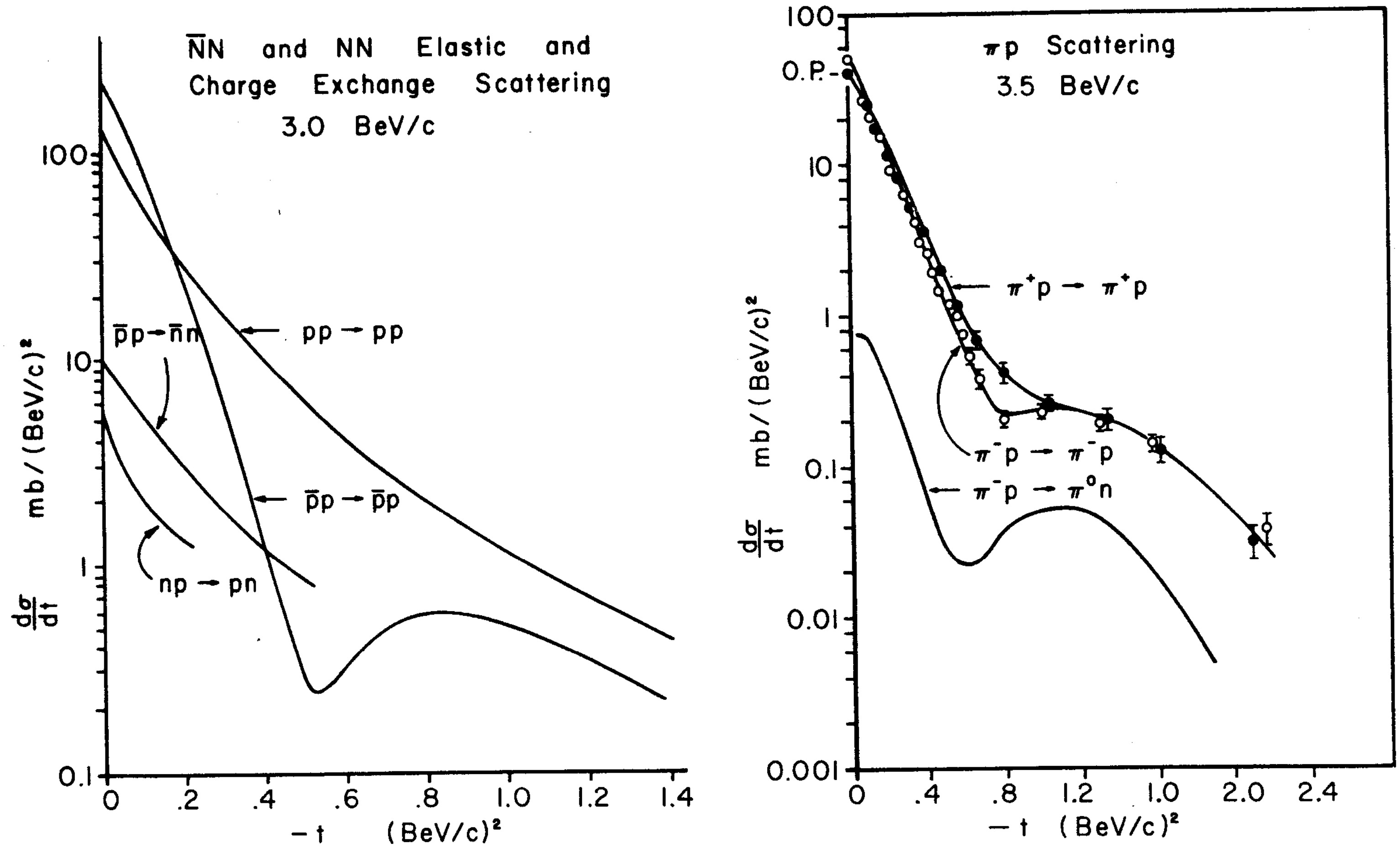

N̄N and NN Elastic and Charge Exchange Scattering 3.0 BeV/c
pp → pp
p̄p → n̄n
p̄p → p̄p
np → pn
dσ/dt mb/(BeV/c)²
−t (BeV/c)²
πp Scattering 3.5 BeV/c
O.P.
π⁺p → π⁺p
π⁻p → π⁻p
π⁻p → π⁰n

FIG. III.1

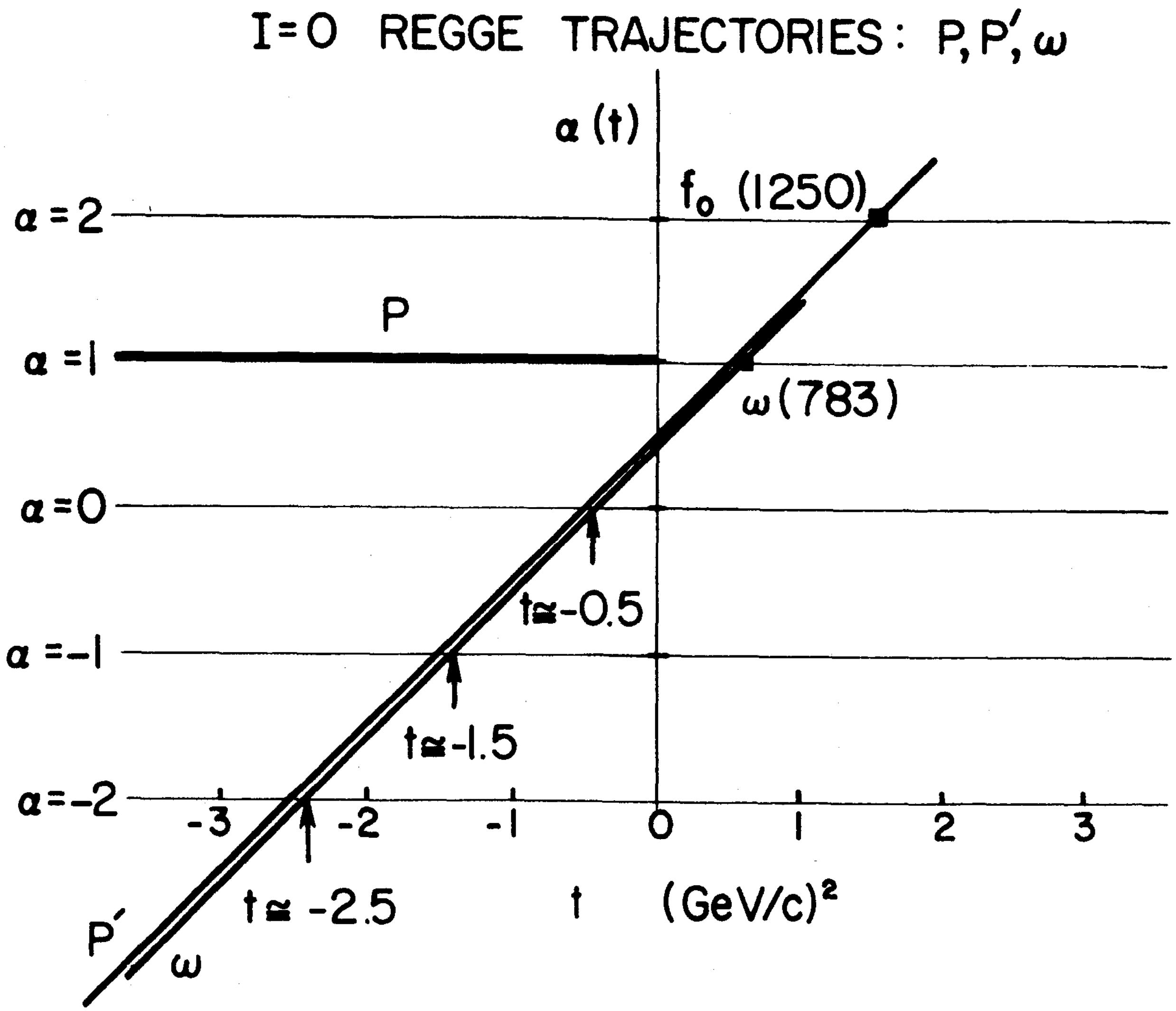

I=0 REGGE TRAJECTORIES: P, P′, ω
α (t)
α = 2
α = 1
α = 0
α = -1
α = -2
P
f_0 (1250)
ω(783)
t≅-0.5
t≅-1.5
t≅ -2.5
-3
-2
-1
0
1
2
3
t (GeV/c)²
P′
ω

FIG. III.2

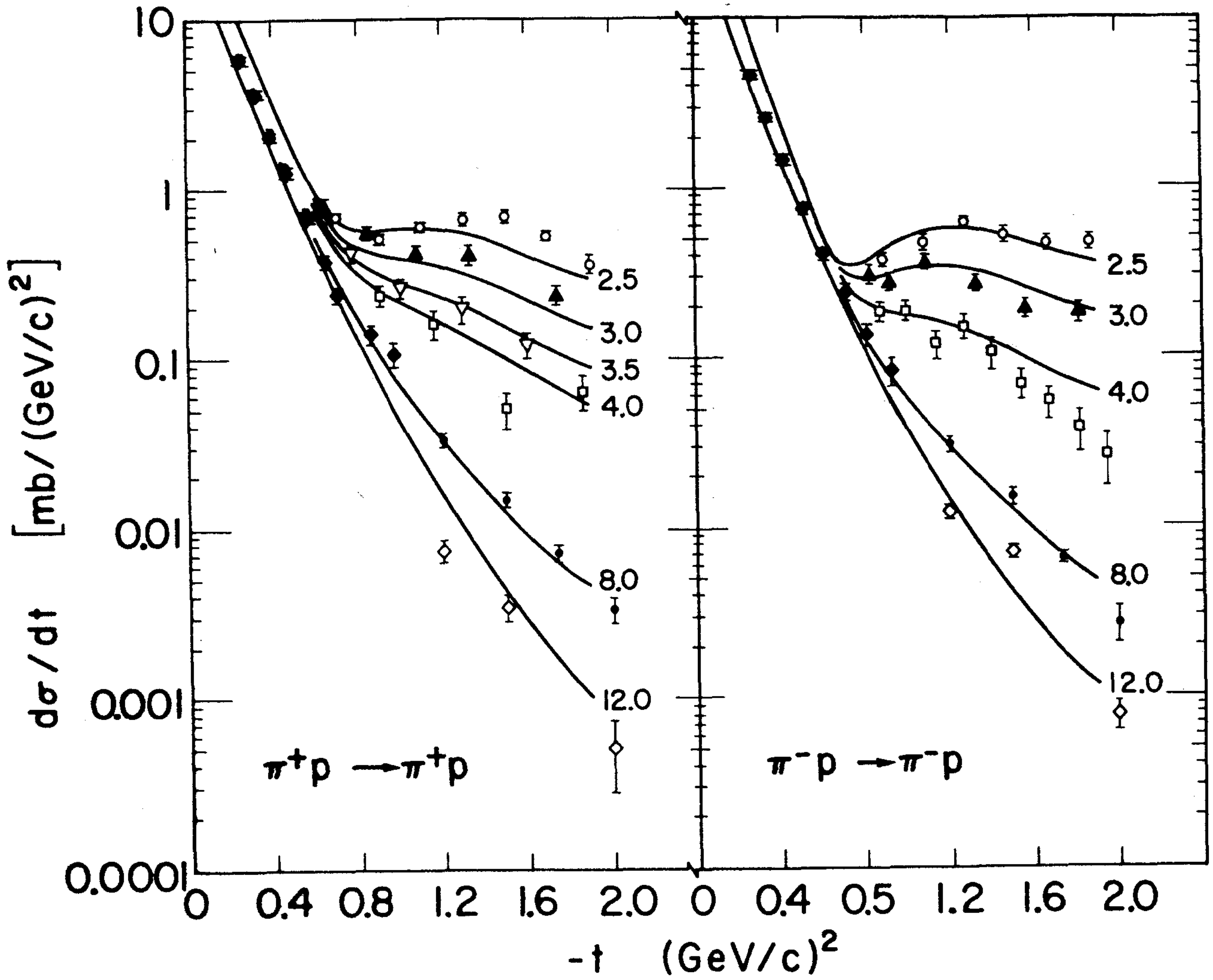
10
1
0.1
0.01
0.001
0.0001
$d\sigma/dt$ [mb/(GeV/c)^2]
2.5
3.0
3.5
4.0
8.0
12.0
$\pi^+ p \rightarrow \pi^+ p$
$\pi^- p \rightarrow \pi^- p$
0 0.4 0.8 1.2 1.6 2.0
0 0.4 0.5 1.2 1.6 2.0
$-t$ (GeV/c)^2

FIG. III.3

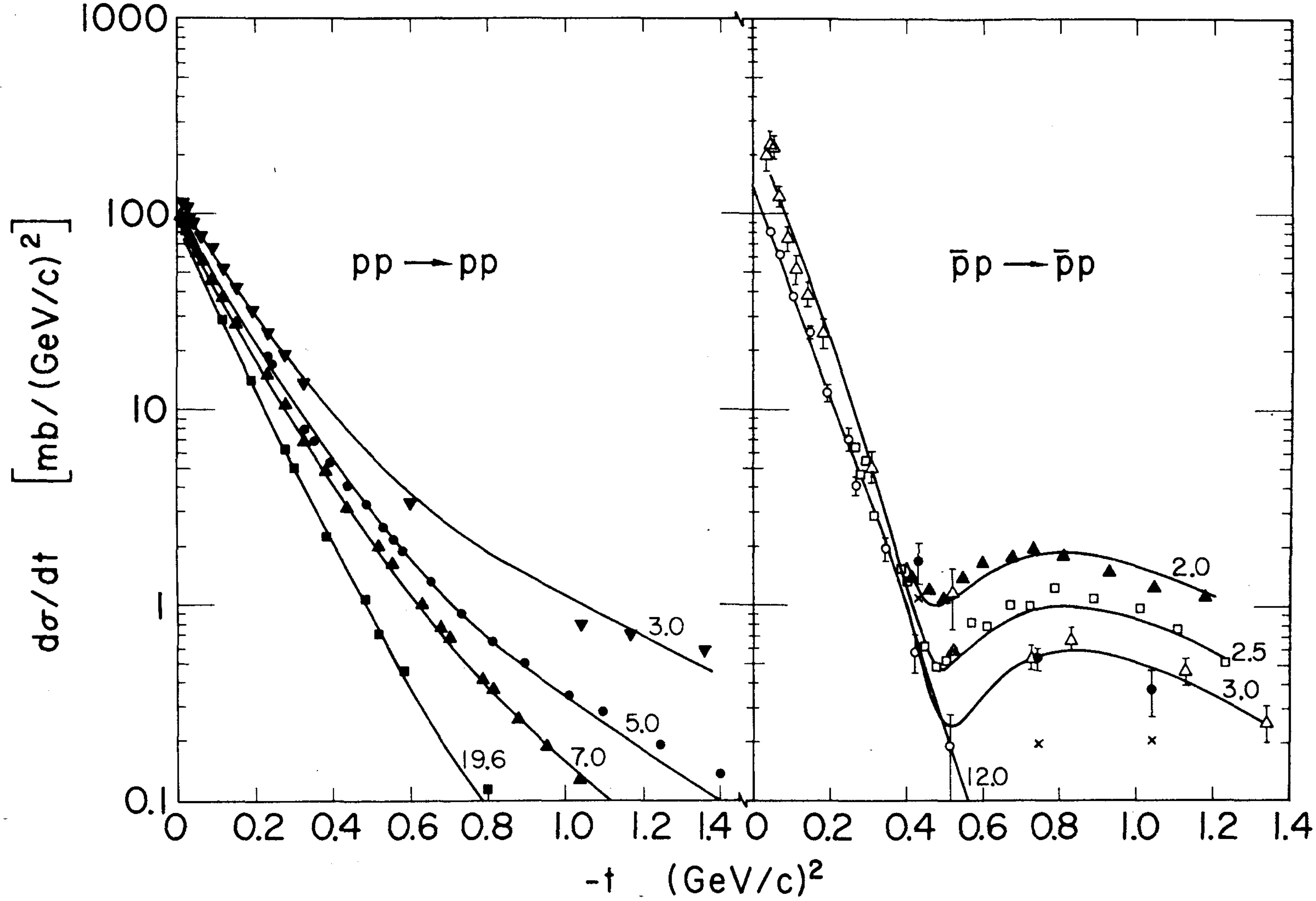

1000
100
10
1
0.1
$d\sigma/dt$ [mb/(GeV/c)^2]
pp → pp
$\bar{p}p \to \bar{p}p$
3.0
5.0
7.0
19.6
2.0
2.5
3.0
12.0
0 0.2 0.4 0.6 0.8 1.0 1.2 1.4
-t (GeV/c)^2

FIG. III.4

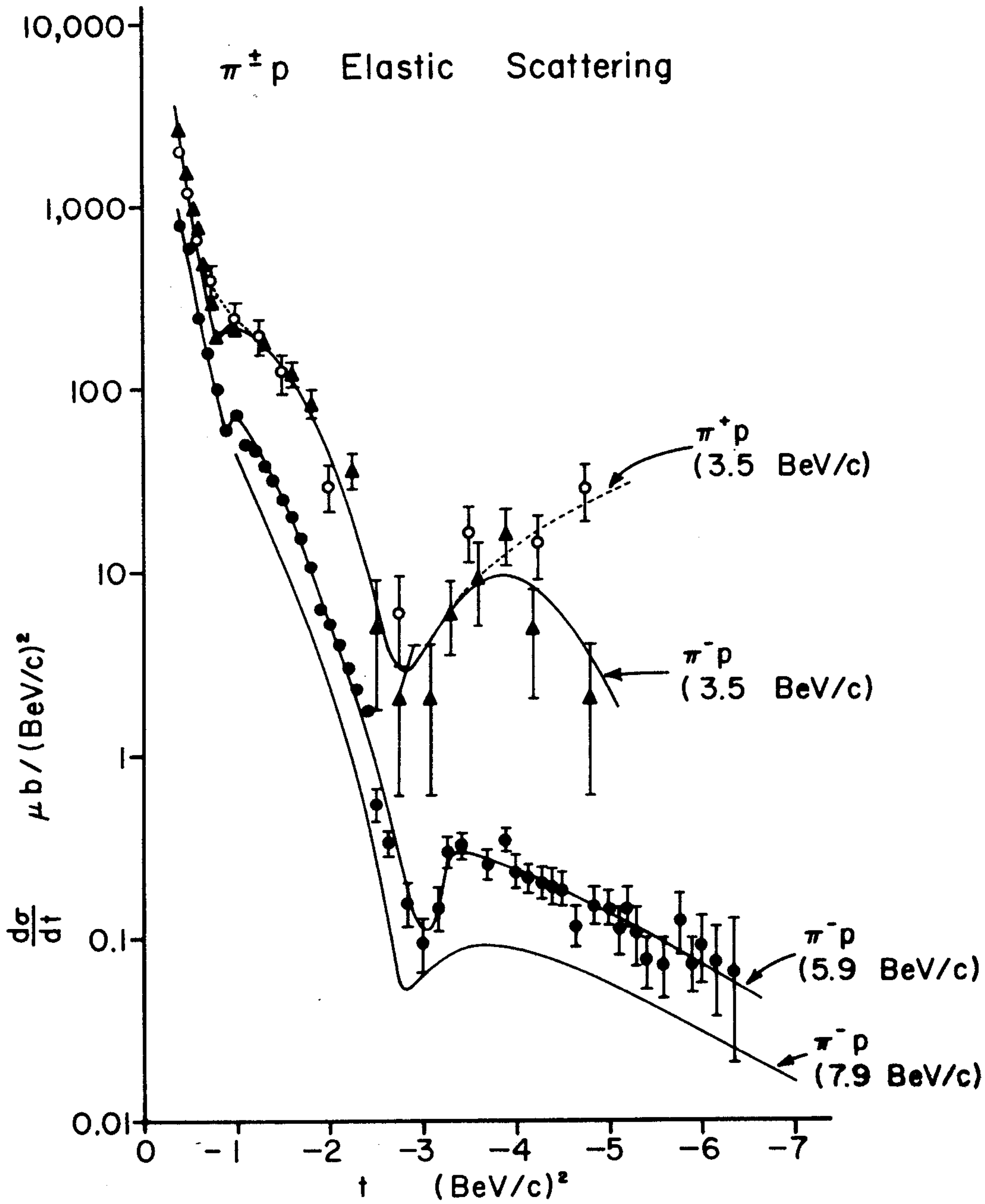
$\pi^{\pm}p$ Elastic Scattering
10,000
1,000
100
10
1
0.1
0.01
$\frac{d\sigma}{dt}$ $\mu b/(BeV/c)^2$
π^+p
(3.5 BeV/c)
π^-p
(3.5 BeV/c)
π^-p
(5.9 BeV/c)
π^-p
(7.9 BeV/c)
0
-1
-2
-3
-4
-5
-6
-7
t (BeV/c)^2

FIG. III.5

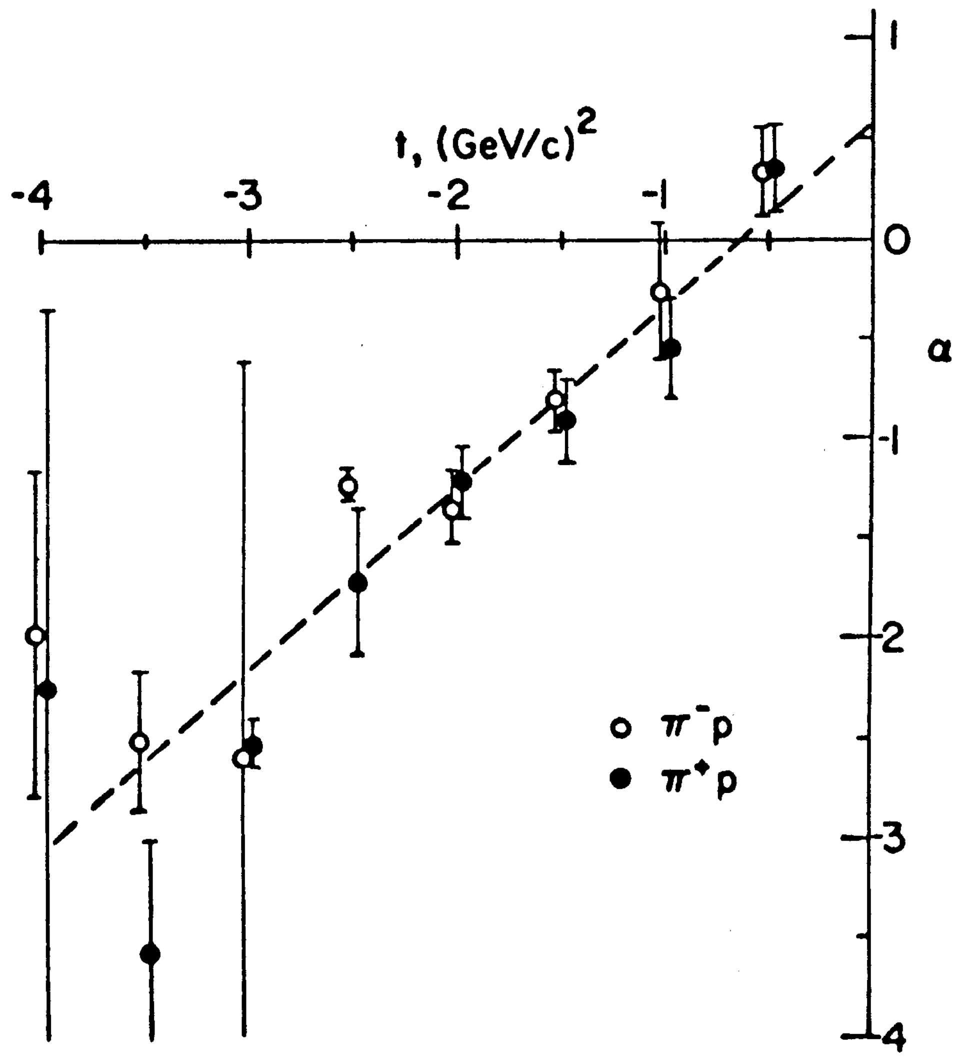

FIG. III .6

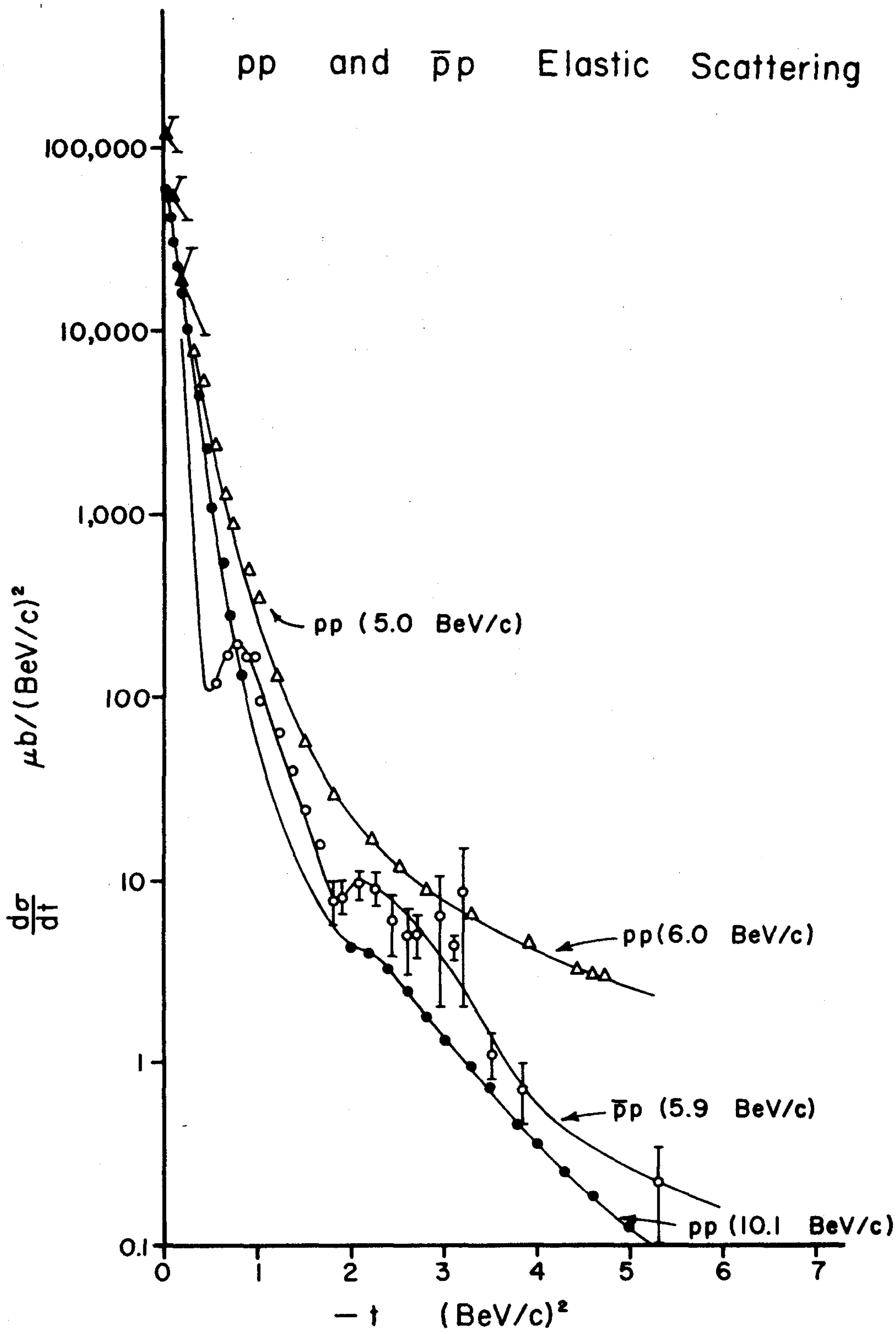

pp and $\bar{p}p$ Elastic Scattering
100,000
10,000
1,000
100
10
1
0.1
$\frac{d\sigma}{dt}$ $\mu b/(BeV/c)^2$
pp (5.0 BeV/c)
pp(6.0 BeV/c)
$\bar{p}p$ (5.9 BeV/c)
pp (10.1 BeV/c)
0
1
2
3
4
5
6
7
$-t$ $(BeV/c)^2$

FIG. III.7